Evolution of surface waviness in thin films via volume and surface diffusion

Rahul Panat, K. Jimmy Hsia, and David G. Cahill

Articles you may be interested in

The effect of a thermal gradient on the electromigration-driven surface morphological stabilization of an epitaxial thin film on a compliant substrate
J. Appl. Phys. **114**, 023503 (2013); 10.1063/1.4812289

The orientation dependent electromigration induced healing on the surface cracks and roughness caused by the uniaxial compressive stresses in single crystal metallic thin films
J. Appl. Phys. **106**, 053503 (2009); 10.1063/1.3211855

Effect of substrate surface on the structure and electronic properties of cubic boron nitride films
J. Appl. Phys. **100**, 014909 (2006); 10.1063/1.2213349

Interdependence between stress, preferred orientation, and surface morphology of nanocrystalline TiN thin films deposited by dual ion beam sputtering
J. Appl. Phys. **99**, 113519 (2006); 10.1063/1.2197287

Surface kinetics and subplantation phenomena affecting the texture, morphology, stress, and growth evolution of titanium nitride films
J. Appl. Phys. **96**, 6234 (2004); 10.1063/1.1811389

Evolution of surface waviness in thin films via volume and surface diffusion

Rahul Panat and K. Jimmy Hsia[a]
Department of Theoretical and Applied Mechanics and the Frederick Seitz Materials Research Laboratory,
University of Illinois, Urbana, Illinois 61801

David G. Cahill
Department of Materials Science and Engineering and the Frederick Seitz Materials Research Laboratory,
University of Illinois, Urbana, Illinois 61801

Deformation mechanisms involving mass transport by stress driven diffusion influence a large number of technological problems. We study the formation of undulations on surfaces of stressed films at high temperature by exploring the deformation kinetics governed by volume and surface diffusion. A governing equation is derived that gives the amplitude change of such surfaces as a function of time. A parametric study is then carried out using a range of practically important input values of the film material properties. The results show that at the dominant instability wavelength, under high average stresses (giga pascal range), only surface diffusion contributes to film surface morphology evolution whereas under low stress and high-temperature conditions, both surface diffusion and volume diffusion contribute to film surface morphology evolution. Furthermore, the contribution of volume diffusion depends on the sign of the film stress, with compressive stress promoting surface roughening and tensile stress promoting surface smoothing. © *2005 American Institute of Physics*. [DOI: 10.1063/1.1827920]

I. INTRODUCTION

Surface morphological instabilities driven by stresses have attracted considerable attention in the last two decades due to their importance in technology. The stability of a solid surface under stress was first addressed by Tiller and co-workers[1,2] while analyzing the role of surface diffusion and surface dissolution and condensation through an adjoining liquid in stress-corrosion cracking. The chemical-potential gradient driving the mass transport processes was assumed to have arisen from the stress variation along the surface and the surface curvature. In their analysis, however, volume diffusion by a vacancy mechanism was neglected since it was believed to be slow at typical temperatures encountered for stress-corrosion cracking. Similar stability analysis was done independently by Grinfeld[3] and Srolovitz.[4] The problem of a stressed solid surface (or surface-vapor interface) becoming unstable at high temperatures was later observed during thin-film growth and annealing.[5–8] The analysis of such instabilities was based on surface diffusion driven by gradients in surface chemical potential,[9–14] an approach that was the same as that of Tiller and co-workers,[1,2] Grinfeld,[3] and Srolovitz.[4]

Although surface diffusion is an important kinetic process, other kinetic processes could affect the evolution of stressed surfaces. One possibility at high temperatures is the diffusion of atoms through the bulk. The chemical-potential gradient driving this volume diffusion would arise due to capillarity[15] and stress variations in the bulk produced by the sinusoidal surface morphology. Note that for unstressed solid

surfaces, capillarity-induced volume fluxes, along with surface diffusion, have been used to predict the decay of surface corrugations by Blakely and co-workers,[16–20] Gjostein and Bonzel,[21] and Liau and Zeiger.[22] Recently, McCarty *et al.*[23] have demonstrated that the smoothing of NiAl surfaces is controlled by the exchange of bulk vacancies with the surface. The relative importance of volume fluxes varies with the temperature and the level of stress.

A simple analysis of the evolution of stressed sinusoidal surfaces of small amplitude is presented in this paper that takes into account (i) surface diffusion driven by gradients in chemical potential along the solid surface and (ii) volume diffusion driven by stress variation along the sinusoidal surface and by capillarity. The governing equations are obtained, followed by a parametric study to reveal the relative importance of the surface and volume diffusion terms. Although this analysis is general, we will compare the model predictions with the waviness formation observed in metallic films of thermal barrier systems.[24]

II. ANALYSIS

Consider a sinusoidal surface of a film over a substrate, as shown in Fig. 1. The system is assumed to be infinitely thick in the z direction so that a plain strain condition exists
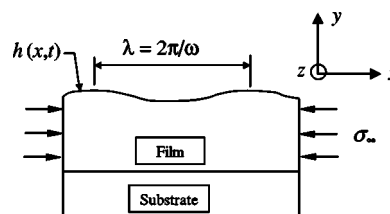

FIG. 1. Sinusoidal perturbations of the free surface of the stressed solid.

[a]Author to whom correspondence should be addressed; current address: Intel Corporation, Assembly Technology Development, CH5-159, Chandler, AZ 85226; FAX: 1(217) 244 5707; electronic mail: kjhsia@uiuc.edu

throughout. The perturbation on the film surface (henceforth referred to as the solid surface) is assumed to take the form

$$h(x,t) = a(t)\cos(\omega x), \tag{1}$$

where a is the perturbation amplitude and $\omega = 2\pi/\lambda$ is the frequency with λ being the perturbation wavelength. An arbitrary solid surface profile can be represented by a Fourier series of such sinusoidal perturbations. The perturbation amplitude of the film surface is assumed to be small compared to its thickness, so that the film can be taken to be infinitely thick while computing the fluxes near the free surface. The slope of the film surface is also assumed to be small, implying $\partial h(x,t)/\partial x \ll 1$ and $\partial/\partial s \approx \partial/\partial x$, where s is the coordinate along the film surface.

A remote stress σ_∞ is applied to the film parallel to the x axis. This stress can arise as a result of differential expansion (or contraction) of the film with the substrate due to thermal-expansion mismatch, phase transformations, differential diffusion of different elements, or defects during deposition.[25–28] We denote σ_∞ positive if compressive. The stress along the solid surface is altered compared to the bulk of the film as a result of the surface perturbation and is given as[1,2,29,30]

$$\sigma_x(x, y = 0) = \sigma_\infty - 2\sigma_\infty a\omega \cos(\omega x). \tag{2}$$

The second term on the right-hand side (RHS) of Eq. (2) represents the *change* in the stress at the solid surface due to the sinusoidal surface geometry. The chemical potential χ along the surface of the wavy solid is[1,13]

$$\chi = (U - \kappa\gamma)\Omega, \tag{3}$$

where κ is the solid surface curvature, Ω is the atomic volume, U is the elastic strain energy per unit volume on the solid surface, and γ is the solid surface energy per unit area, assumed to be isotropic.

The strain energy density at the surface, U is given by

$$U(x,t) = \frac{(1-\nu)\sigma_\infty^2}{4G}[1 - 4a\omega\cos(\omega x)], \tag{4}$$

where G is the shear modulus. In writing Eq. (4), the higher-order terms of $a\omega$ are neglected as a result of the small slope assumption. If the film in Fig. 1 was not attached to the substrate and free to move, the wavelength λ would be a function of time. For a film attached to the substrate, however, it is reasonable to assume that planes remain as planes in the film during surface evolution.[31] In such a case, $h(x,t) = a(t)\cos(\omega x)$, i.e., the fluctuation amplitude alone varies with time. The chemical-potential change along the surface drives atom diffusion, giving rise to a flux along the surface (Fig. 2, also see Asaro and Tiller[1])

$$J_s = -\frac{D_s C_s}{kT}\frac{\partial\chi}{\partial x}$$

$$= \frac{D_s C_s \Omega \sin(\omega x)}{kT}\left[\frac{(1-\nu)\sigma_\infty^2}{G}a\omega^2 - \gamma a\omega^3\right], \tag{5}$$

where D_s is the surface self-diffusivity, C_s is the number of diffusing atoms per unit area, k is the Boltzmann constant,
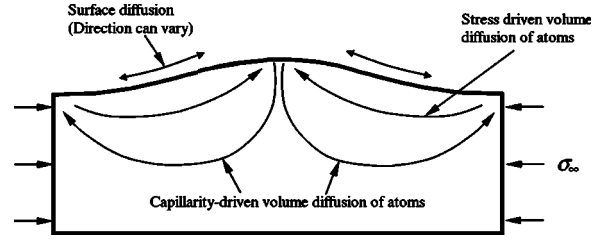

FIG. 2. A portion on the film surface between two troughs showing various diffusion processes.

and T is the absolute temperature. In writing Eq. (5), we have taken κ to be $\partial^2 h(x,t)/\partial x^2$.

For a film under mechanical equilibrium, the pressure (hydrostatic stress) just below the film surface varies according to two independent "loading" parameters: capillarity (surface tension) and the applied remote stress, as explained in the Appendix. Fractional vacancy concentration as a result of the pressure variation just below the surface is given by Eq. (A3). This vacancy concentration, $C(x, y = 0)$, is different from that far below the surface, which is the equilibrium concentration C_v at a given temperature T and average stress σ_∞. We take the vacancy concentration variation in the film to be[15]

$$C(x,y) = C_v + \frac{C_v\Omega}{kT}$$

$$\times\left[-a\omega^2\gamma + \frac{2}{3}(1+\nu)\sigma_\infty a\omega\right]\cos(\omega x)e^{\omega y}. \tag{6}$$

It can be shown that the vacancy concentration given by Eq. (6) satisfies the Laplace equation, $\nabla^2 C = 0$ everywhere in the body. Therefore, sources and sinks of vacancies need only exist along the surface of the film.

The concentration gradient in the vacancies in the y direction will result in a vacancy flux at the film surface (Fig. 2),

$$J_v = -D_v\frac{\partial[C(x,y)/\Omega]}{\partial y}\bigg|_{y=0}$$

$$= \frac{D_v C_v}{kT}\left[\gamma\omega^3 - \frac{2(1+\nu)}{3}\sigma_\infty\omega^2\right]a\cos(\omega x), \tag{7}$$

where D_v is the vacancy self-diffusivity. Note that for most metals, the product, $D_v C_v$, is equal to the volume self-diffusivity of the solid, D_1. We replace $D_v C_v$ by D_1 in the current analysis. While writing Eq. (7), the gradient of vacancy concentration normal to the surface is approximated as $\partial[C(x,y)/\Omega]/\partial y$ and computed at $y = 0$ due to the small slope assumption.[15] The first term in Eq. (7) implies that a net flux of atoms flows from the crests to the troughs (Fig. 2) as a result of a net flux of vacancies from the troughs to the crests. Thus, the vacancy flux due to the first term in Eq. (7) tends to flatten the surface profile. For a compressive remote stress, the second term of Eq. (7) will cause the troughs to experience a flux of vacancies along the positive y axis and vice versa. Such a flux would roughen the film surface.

The surface and volume diffusion described above are assumed to take place in the region close to the surface and
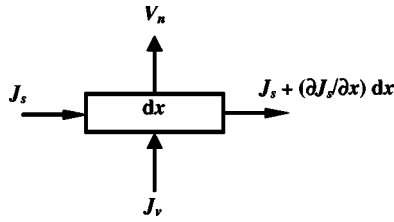
FIG. 3. Diffusion along an element of the surface.

hence the volume flux at the surface can be used to compute the velocity of the surface, as shown in Fig. 3. Conservation of mass at a surface element (Fig. 3) gives the normal velocity

$$V_n = \frac{\partial h(x,t)}{\partial t} = -\Omega \frac{\partial J_s}{\partial x} + \Omega(-J_v). \tag{8}$$

The rate of change of fluctuation amplitude can then be computed from the definition of $h(x,t)$, along with Eqs. (5), (7), and (8) as

$$\frac{1}{a(t)}\frac{da(t)}{dt} = \frac{D_{s0}C_{s0}\Omega^2}{kT}e^{-q_s/kT}\left[\frac{(1-\nu)\sigma_\infty^2}{G}\omega^3 - \gamma\omega^4\right]$$
$$+ \frac{D_{10}\Omega}{kT}e^{-q_1/kT}\left[\frac{2(1+\nu)}{3}\sigma_\infty\omega^2 - \gamma\omega^3\right]. \tag{9}$$

Here, D_sC_s and D_1 are replaced by $D_{s0}C_{s0}\exp(-q_s/kT)$ and $D_{10}\exp(-q_1/kT)$, with q_s and q_1 being the corresponding activation energies. The first term in Eq. (9) tends to roughen the surface, irrespective of the sign of remote stress, while the third term roughens the surface only for compressive remote stress. The ω^2 (or $1/\lambda^2$) dependence of the third term in Eq. (9) is similar to the $1/(\text{grain size})^2$ dependence of the strain rate[32] during creep of a polycrystalline material. Note that the rate of the amplitude increase per unit amplitude $[(1/a)(da/dt)]$ in the present problem is thus analogous to the creep strain rate.

The second and the fourth terms in Eq. (9) represent the tendency of the sinusoidal surface to flatten. In the absence of remote stresses, we go back to the case described by Mullins[15] where the surface *always* flattens through diffusion at high temperatures. The decay constant during corrugation smoothing[16–22] is now replaced by a "decay" or an "amplification" constant depending upon the surface undulation frequency. The terms in Eq. (9) that have the most influence on the surface evolution at a given ω include $D_1/(D_sC_s)$ and σ_∞. We carry out this analysis in Sec. III by taking input values for the variables in Eq. (9) from the literature.

III. RESULTS AND DISCUSSION

We start by analyzing Eq. (9) for constant temperature as applied in various experimental studies of surface evolution of stressed[7,24] and unstressed surfaces.[16–20] First, a brief literature survey of the typical values of the relevant parameters in Eq. (9) is presented, especially those pertaining to the thermal barrier systems. The remote stress (σ_∞) in the films can vary widely. In films of thermal barrier systems, this stress is in tens of mega pascals at high

temperatures.[33–35] In other thin-film roughening experiments, this stress could be in the giga pascal range.[8,13,29]

Few q_1 values for Ni-based bond coat alloys used in thermal barrier systems and related materials have been reported in literature. For NiAl, the activation energy for interdiffusion, q_1, of 2.71–3.25 eV (Ref. 35) has been reported. The q_1 for Ni is about 2.89 eV.[36] For surface diffusion, the reported q_s values for Ni vary considerably, from 0.82 eV (Ref. 21) to 1.54–1.85 eV.[18] This variation is due to surface conditions and surface orientation. To the authors' knowledge, q_s for metal film surfaces in thermal barrier systems has not been experimentally determined. The ratio of $D_1/(D_sC_s)$ can thus vary over a few orders of magnitude depending upon conditions such as crystal orientation, temperature, and surface cleanliness. For Ni, the ratio $D_1/(D_sC_s)$ was reported to be about 1.5×10^{-25} m^2 at 1273 K and 1.8×10^{-24} m^2 at 1473 K by some researchers,[21,36] and was reported to vary from 2.5×10^{-25} to 10^{-24} m^2 at 1273 K and 1.3×10^{-24} to 3.7×10^{-24} m^2 at 1473 K by others.[18,36] For Cu, $D_1/(D_sC_s)$ has been reported to be 1.3×10^{-24} m^2 at 1273 K[36,37] while for α-Fe, this ratio is about 10^{-24} m^2 at all temperatures.[38]

The surface energy γ of the film is typically of the order of 1 J/m^2. The isothermal (annealing) temperature for roughening experiments in thermal barrier systems is between 1373 and 1473 K.[24,39–41] Note that the effect of the isothermal temperature on our results is incorporated through the ratio $D_1/(D_sC_s)$.

To gain an insight on the film surface roughening through combined surface and volume diffusion, we find the amplitude change of surface perturbations with time as a function of wavelength from Eq. (9) for a set of input parameters given below. For $G=100$ GPa, $\nu=1/3$, $\sigma_\infty=25$ MPa, $D_1/(D_sC_s)=10^{-25}$ m^2, $\gamma=1$ J/m^2, and $\Omega=4.29\times10^{-29}$ m^3 (Blakely and Mykura[42] for Ni), Eq. (9) gives

$$\ln\left[\frac{a(t)}{a_0}\right]\Big|_{\hat{\lambda}} = \frac{8\pi^3 D_sC_s\Omega^2\sigma_\infty^6 t}{kT\gamma^3 G^3}\hat{\lambda}^{-3}(P - Q\hat{\lambda}^{-1} + R\hat{\lambda} - S), \tag{10}$$

where P, Q, R, and S are parameters equal to 4.2×10^3, 3.9×10^4, 1.3×10^6, and 2.3×10^3 N/m^2, respectively, for the chosen set of material parameters, $\hat{\lambda}=2\pi\sigma_\infty^2/(\omega\gamma G)$ is the dimensionless wavelength, a(t) is the fluctuation amplitude at time t, while a$_0$ is the initial amplitude.

The normalized amplitude change of the film, a(t)/a$_0$, as a function of wavelength λ from Eq. (10) is plotted in Fig. 4(a). The plot reveals different rates of amplitude change for perturbations of different wavelengths. For surface undulations with wavelengths less than a critical value, λ_{cr} [Fig. 4(a)], the amplitude decreases with time. This value is about 28 μm in the present case. It can be seen that in this region ($\lambda < \lambda_{cr}$), the logarithm of the amplitude ratio is negative, i.e., the amplitude decreases rapidly as the wavelength of waviness decreases. On the other hand, undulations with wavelength greater than λ_{cr} increase in amplitude at varying relative rates with time. The result also shows that the maximum amplitude change occurs at a wavelength λ_{max} [Fig. 4(a)] of about 38 μm in the present case. The components
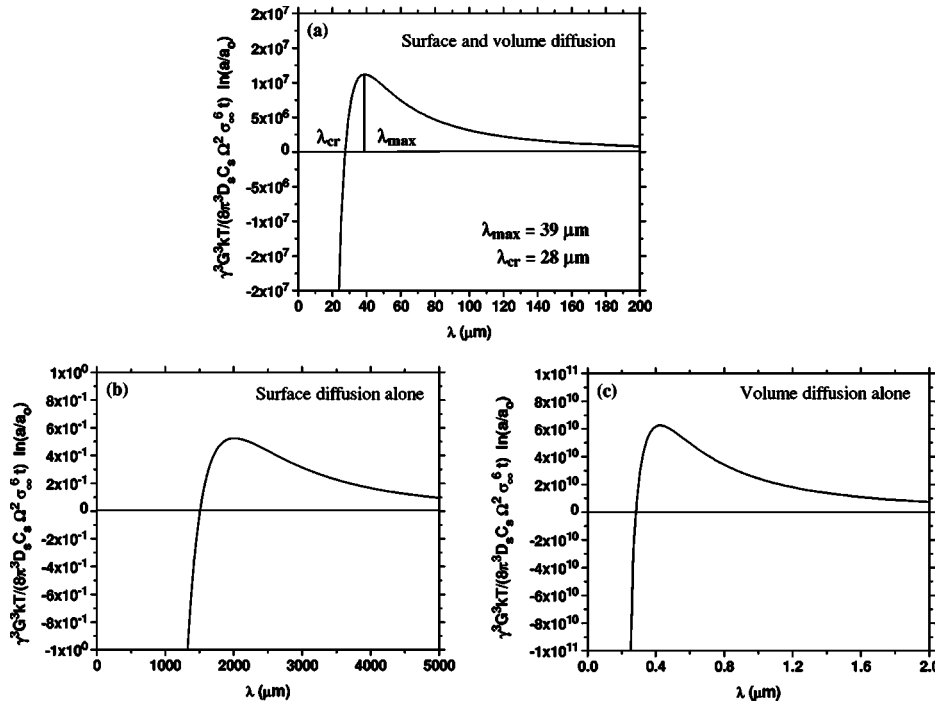
FIG. 4. Ratio of amplitude change of a film as a function of wavelength for isothermal temperature history. (a) Considering both surface and volume diffusion, (b) considering surface diffusion alone [first two terms on RHS of Eq. (9)], and (c) considering volume diffusion alone [last two terms on RHS of Eq. (9)].

with wavelengths close to this peak point grow faster than the components of other wavelengths. The evolution of the film described by Fig. 4(a) is qualitatively similar to that if we consider surface diffusion alone, as shown in Fig. 4(b) (also see Asaro and Tiller[1] and Freund[13]) or volume diffusion alone, as shown in Fig. 4(c). However, the critical and the maximum wavelengths are significantly larger when considering surface diffusion alone (about 1510 and 2010 μm, respectively) or considerably smaller when considering volume diffusion alone (about 0.28 and 0.42 μm, respectively). Thus, for the set of parameters used to plot Fig. 4, neither of the two diffusion paths alone can explain the waviness formation seen in thermal barrier systems[24] where the wavelength of waviness is seen to be tens of micrometers.

Figure 4 suggests that given enough time to evolve, the film surface wavelengths should be relatively independent of the initial surface features and be dominated by wavelengths close to λ_{max}. For the material parameters used to obtain Fig. 4, the contribution to roughening by the first term and the contribution to smoothing by the fourth term in Eq. (9) are negligible compared to those by the third term and the second term at λ_{max}. At λ_{max} for the material parameters considered, the only destabilizing mechanism for the surface perturbations is volume diffusion, while the only stabilizing mechanism is surface diffusion. Under these conditions,

$$\lambda_{max} = \sqrt{2}\lambda_{cr} = 2\pi\left[\frac{3\Omega\gamma}{(1+\nu)\sigma_\infty}\frac{D_sC_s}{D_1}\right]^{1/2}. \quad (11)$$

The value of λ_{max} as a function of $D_1/(D_sC_s)$ and stress σ_∞ is shown in Fig. 5. Other parameters used to plot Fig. 5 are the same as those used for Fig. 4(a). The dominant surface wavelength in Fig. 5(a) increases with decreasing volume diffusion relative to surface diffusion [i.e., decreasing

$D_1/(D_sC_s)$]. Figure 5(a) also shows that the values of λ_{max} decrease with increasing stress at a given relative diffusional rate, $D_1/(D_sC_s)$. This is due to the fact that the λ_{max} predicted by surface diffusion alone in Eq. (9) decreases faster with stress (proportional to σ_∞^2) compared to that predicted by volume diffusion alone (proportional to σ_∞).

Results similar to Fig. 5(a) are plotted in Fig. 5(b) for low stress levels. Figure 5(b) shows that the inclusion of volume diffusion terms has a considerable effect on the value
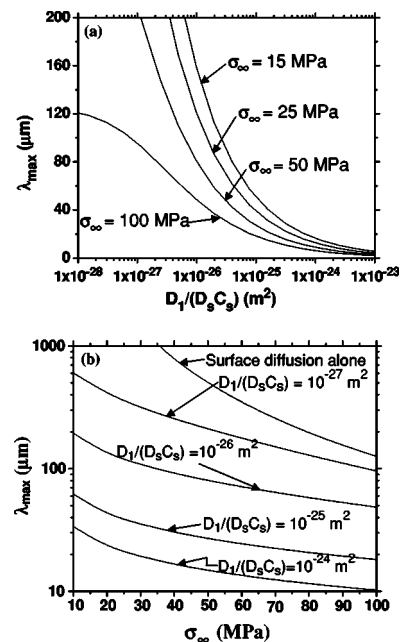

FIG. 5. The λ_{max} of a film as (a) a function of $D_1/(D_sC_s)[=D_vC_v/(D_sC_s)]$ at several compressive stress levels and as (b) a function of stress for several values of $D_1/(D_sC_s)$.
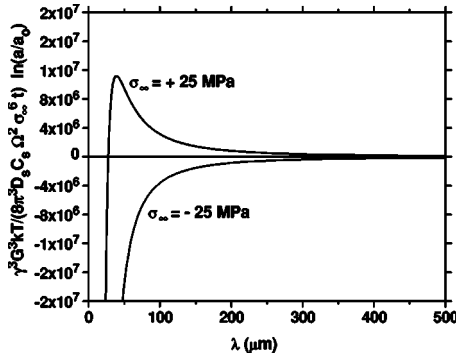
FIG. 6. Ratio of amplitude change of a film as a function of wavelength under compressive (+25 MPa) and tensile (−25 MPa) stresses. Note that the surface roughens under compressive stress but smoothens under tensile stress.

FIG. 8. The λ_{max} of a film as a function of tensile and compressive remote stresses for different $D_1/(D_s C_s)$ values.

of λ_{max} (y axis has a logarithmic scale) when the film remote stress is low. At high stress levels in giga pascal range though, the effect of volume diffusion would be insignificant (see Fig. 8), in line with previous analyses.[9,10,12,13,30] The effect of temperature on λ_{max} can be qualitatively assessed from Fig. 5. As the annealing temperature decreases, the ratio $D_1/(D_s C_s)$ decreases since q_s is smaller than q_1. Hence, a decreasing temperature is equivalent to a decreasing $D_1/(D_s C_s)$ in Fig. 5. The rate of this decrease depends on (q_1-q_s).

One significant feature of the current analysis is that, unlike that predicted by considering surface diffusion alone,[1,3,4,9,10,12–14] the film roughening is sensitive to the sign of the remote stress. Under remote compressive stress (Figs. 4 and 5), volume diffusion driven by the remote stress tends to roughen the film surface while that due to surface tension (i.e., γ) tends to smoothen the film surface. Their competition gives rise to surface roughening at λ_{max}. Under remote tensile stress, however, both volume diffusion and surface tension tend to smoothen the surface perturbations [see Eq. (9)]. At low tensile stresses, volume diffusion, and hence this effect, is dominant, as illustrated in Fig. 6, which shows that compressive stress causes the surface to roughen while tensile stress does not. As the tensile stress increases, roughening due to surface diffusion increasingly dominates over flattening due to volume diffusion. Figure 7 shows the normalized surface-roughening rate at λ_{max} as a function of remote tensile stress, which demonstrates that, when the magnitude of the remote tensile stress is large, the film sur-
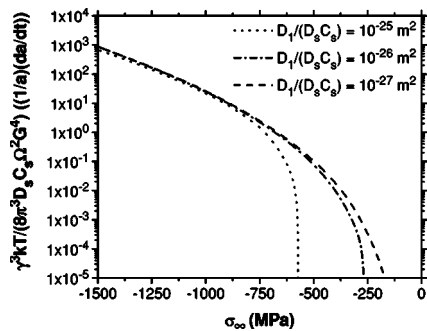

FIG. 7. Normalized surface-roughening rate as a function of remote tensile stress at the wavelength λ_{max}.
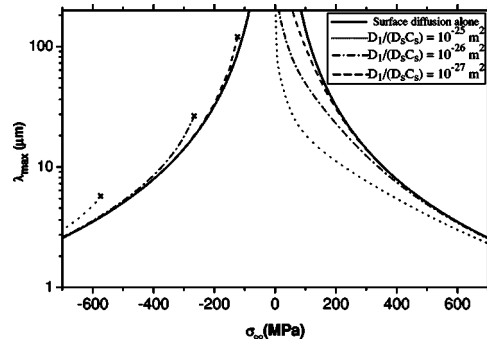
face roughens at a high rate and vice versa. For a given volume to surface diffusivity ratio, there exists a critical stress magnitude below which no roughening occurs. The stress-sign dependence of the surface-roughening behavior is a direct consequence of the vacancy concentration variation induced by pressure variation along a wavy surface. While a remote compressive stress will increase the pressure at valleys and decrease it at crests of a wavy surface, as shown in Fig. 2, a remote tensile stress will give rise to the opposite.

The difference in λ_{max} under compressive and tensile remote stresses can be more clearly seen in Fig. 8. Figure 8 shows that, with surface diffusion alone, the dependence of λ_{max} on stress levels is symmetric, i.e., λ_{max} depends only upon the magnitude of the remote stress. However, inclusion of volume diffusion lowers the values of λ_{max} under compressive remote stress and increases the values of λ_{max} under tensile remote stress. Further, the current analysis indicates that under tensile remote stress with volume diffusion, roughening will not occur when the stress magnitude is below a critical value, indicated by the terminating points in Fig. 8. This is not the case under a compressive remote stress. This asymmetric surface-roughening behavior under tensile and compressive remote stresses has not been predicted previously. It may be partly responsible for the experimental observations of different behaviors in isothermal testing done below and above the processing temperature in the films of thermal barrier systems.[41,43] Similar asymmetric behavior has been predicted by a linear stability analysis of viscous fingering of the interface between two linearly creeping fluids of different viscosity.[44] Figure 8 also shows that, as the magnitude of the remote stress increases, the influence of volume diffusion diminishes regardless of the sign of the remote stress.

The prerequisite for the current analysis to be valid is the existence of a sustainable average stress in the thin film during surface morphology evolution. In epitaxial thin films, such stress is maintained because of lack of sources and sinks for point defects so that stress relaxation is difficult to occur. In the coatings of thermal barrier systems (i.e., bondcoat), the maintenance of a relatively low stress level at elevated temperatures may be attributed to the fact that the characteristic relaxation time due to volume diffusion is much longer than the time required for surface morphology evolution. Pan et al.[35] showed that, in free-standing bondcoat tested at high temperatures, the stresses relaxed immediately

after straining, likely due to dislocation creep. After the initial drop, the stresses settled to a long period of nearly constant level. Such sustained stress over a sufficiently long period would be able to provide the driving force for surface roughening in these coatings. Moreover, in thermal barrier systems, continued interdiffusion between bondcoat and substrate may also induce stresses in the bondcoat, similar to the mechanism analyzed by Suo et al.[27]

It is also important to know whether the current analysis is capable of confirming the profound amplitude increases during surface roughening of thin films.[8,24] Some estimates can be made for the amplitude change predicted by the current model. For conditions used to plot Fig. 5, when the remote stress is 25 MPa, λ_{max} is about 20 μm [i.e., $D_1/(D_s C_s) = 3.9 \times 10^{-25}$ m^2] and $D_{s0} \exp[-q_s/(kT)]$ is 5 $\times 10^{-9}$ m^2/s, we get $\ln(a/a_0) = 3.62 \times 10^{-5} t$ (t in seconds). Thus the exponential growth time of the instability is approximately 8 h, small compared to the 25-h isothermal heating in the experiments of Panat et al.[24] and Panat and Hsia.[41]

IV. CONCLUSIONS

In this paper we present an analysis describing the evolution of sinusoidal surfaces of stressed films by considering the diffusion of atoms through the film volume and along the film surface. Volume diffusion is shown to be influential at the relatively low stress levels (tens of mega pascals) typically encountered in films in thermal barrier systems while not important at high stress levels (giga pascal range). The relative importance of volume diffusion is also controlled by the ratio of the volume self-diffusivity to the product of the surface self-diffusivity with the surface defect concentration. The inclusion of volume diffusion terms in the stability analysis implies a different behavior of the film surfaces under a tensile and a compressive stress. This effect is, however, shown to affect the stability only at low stress levels. The current study shows that, at the dominant instability wavelength and under low stress and high-temperature conditions, the only important destabilizing mechanism is volume diffusion, while the only important stabilizing mechanism is surface diffusion.
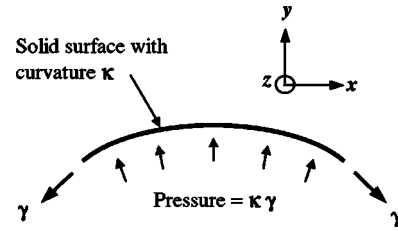
FIG. 9. Curved solid surface.

APPENDIX

Consider a curved solid surface of curvature κ in the x-y plane, as shown in Fig. 9. Simple mechanical equilibrium shows that a pressure difference (i.e., hydrostatic stress) equal to $\kappa\gamma$ will develop in the solid just below the surface, where γ is the solid surface energy (assumed to be isotropic and same as surface tension).[45] For a crest on the solid surface, the pressure is compressive and vice versa. The fractional concentration of vacancies just below the surface due to this pressure is given by[15]

$$C' = C_v' + \frac{C_v' \gamma \Omega}{kT} \kappa, \tag{A1}$$

where C_v' is the concentration of vacancies in equilibrium with a flat solid surface.

In the case of the surface of a film under a remote stress (Fig. 1), an additional hydrostatic stress is superimposed over that due to capillarity. Since the surface of the solid is curved, this stress can vary along the x axis. Let us consider a film with its surface morphology given by Eq. (1) and under a remote stress σ_∞, as shown in Fig. 1. The hydrostatic pressure due to the remote stress can be evaluated as $(1/3) \times (\sigma_{xx} + \sigma_{yy} + \sigma_{zz})$ at $y=0$. Using Eq. (2) and assuming a plane strain condition, the difference between the hydrostatic pressure at the sinusoidal surface of the film in Fig. 1 and that of a flat surface is

$$\Delta P = \frac{-2}{3}(1+\nu)\sigma_\infty a\omega \cos(\omega x). \tag{A2}$$

This pressure difference between the film surface and film interior, which varies along x, serves the same role in affecting the vacancy concentration as the pressure variation due to capillarity.

By finding a steady-state solution of the volume diffusion problem for vacancies, the concentration of vacancies just below the surface, C, due to the combined effect of surface tension and remote stress can be given by

$$C(x, y = 0) = C_v + \frac{C_v \Omega}{kT}$$
$$\times \left[-a\omega^2 \gamma + \frac{2}{3}(1+\nu)\sigma_\infty a\omega \right] \cos(\omega x), \tag{A3}$$

where C_v is the concentration of vacancies in equilibrium with a flat surface of a film under a remote stress. Thus, the equilibrium vacancy concentration in the bulk of the film in Fig. 1 (i.e., far below the surface) is given by C_v. Note that in

writing Eq. (A3), we assume that the vacancy volume is the same as the atomic volume.[15,16]

[1]R. J. Asaro and W. A. Tiller, Metall. Trans. **3**, 1789 (1972).
[2]P. Vasudev, R. J. Asaro, and W. A. Tiller, Acta Metall. **23**, 341 (1975).
[3]M. A. Grinfeld, J. Nonlinear Sci. **3**, 35 (1993).
[4]D. J. Srolovitz Acta Metall. **37**, 621 (1989).
[5]F. K. LeGoues, M. Copel, and R. M. Tromp, Phys. Rev. B **42**, 11690 (1990).
[6]D. F. Jesson, S. Pennycook, J. M. Baribeau, and D. C. Houghton, Phys. Rev. Lett. **71**, 1744 (1993).
[7]C. S. Ozkan, W. D. Nix, and H. Gao, Appl. Phys. Lett. **70**, 2247 (1997).
[8]H. Gao and W. D. Nix, Annu. Rev. Mater. Sci. **29**, 173 (1999).
[9]R. Bruinsma and A. Zangwill, Europhys. Lett. **4**, 729 (1987).
[10]B. J. Spencer, P. W. Voorhees, and S. H. Davis, Phys. Rev. Lett. **67**, 3696 (1991).
[11]H. Gao, J. Mech. Phys. Solids **42**, 741 (1994).
[12]L. B. Freund and F. Jonsdottir, J. Mech. Phys. Solids **41**, 1245 (1993).
[13]L. B. Freund, Int. J. Solids Struct. **32**, 911 (1995).
[14]J. Colin, J. Grilhe, and N. Junqua, J. Phys. IV **8**, Pr4 (1998).
[15]W. W. Mullins, in *Metal Surfaces*, edited by W. D. Robertson and N. A. Gjostein (American Society for Metals, Metals Park, OH, 1963), pp. 17–66.
[16]J. M. Blakely and H. Mykura, Acta Metall. **10**, 565 (1962).
[17]P. S. Maiya and J. M. Blakely, Appl. Phys. Lett. **7**, 60 (1965).
[18]P. S. Maiya and J. M. Blakely, J. Appl. Phys. **38**, 698 (1967).
[19]D. L. Olson, H. R. Patil, and J. M. Blakely, Scr. Metall. **6**, 229 (1972).
[20]M. F. Keefe, C. C. Umbach, and J. M. Blakely, J. Phys. Chem. Solids **55**, 965 (1994).
[21]N. A. Gjostein and H. P. Bonzel, J. Appl. Phys. **39**, 3480 (1968).
[22]Z. L. Liau and H. J. Zeiger, J. Appl. Phys. **67**, 2434 (1990).
[23]K. F. McCarty, J. A. Nobel, and N. C. Bartelt, Nature (London) **412**, 622 (2001).
[24]R. P. Panat, K. J. Hsia, and J. Oldham, Philos. Mag. in press (2004).
[25]M. D. Thouless, Annu. Rev. Mater. Sci. **25**, 69 (1995).
[26]M. W. Chen, R. T. Ott, T. C. Hufnagel, P. K. Wright, and K. J. Hemker, Surf. Coat. Technol. **163–164**, 25 (2003).
[27]Z. Suo, D. Kubair, A. G. Evans, D. R. Clarke, and V. Tolpygo, Acta Mater. **51**, 959 (2003).
[28]S. Zhang, H. T. Johnson, G. J. Wagner, W. K. Liu, and K. J. Hsia, Acta Mater. **51**, 5211 (2003).
[29]H. Gao, Int. J. Solids Struct. **28**, 703 (1991).
[30]H. Gao, J. Mech. Phys. Solids **39**, 443 (1991).
[31]M. D. Thouless, Acta Metall. Mater. **41**, 1057 (1993).
[32]P. G. Shewmon, *Diffusion in Solids* (Minerals, Metals & Materials Society, Warrandale, PA, 1989), chap. 6, pp. 208–213.
[33]R. P. Panat, S. Zhang, and K. J. Hsia, Acta Mater. **51**, 239 (2003).
[34]A. M. Karlsson and A. G. Evans, Acta Mater. **49**, 1793 (2001).
[35]D. Pan, M. W. Chen, P. K. Wright, and K. J. Hemker, Acta Mater. **51**, 2205 (2003).
[36]D. A. Porter and K. E. Easterling, *Phase Transformations in Metals and Alloys* (Van Nostrand Reinhold, New York, 1981).
[37]J. Y. Choi and P. G. Shewmon, Trans. Metall. Soc. AIME **224**, 589 (1962).
[38]J. M. Blakely and H. Mykura, Acta Metall. **11**, 399 (1963).
[39]P. Deb, D. H. Boone, and T. F. I. Manley, J. Vac. Sci. Technol. A **5**, 3366 (1987).
[40]V. K. Tolpygo and D. R. Clarke, Acta Mater. **48**, 3283 (2000).
[41]R. P. Panat and K. J. Hsia, Proc. R. Soc. London, Ser. A **460**, 1957 (2004).
[42]J. M. Blakely and H. Mykura, Acta Metall. **9**, 23 (1961).
[43]R. P. Panat, Ph.D. thesis, University of Illinois at Urbana–Champaign, 2004.
[44]F. Sherman, *Viscous Flow* (McGraw-Hill, New York, 1990).
[45]C. Herring, in *Structure and Properties of Solid Surfaces*, edited by R. Gomre and C. S. Smith (University of Chicago Press, Chicago, 1953), pp. 1–81.